

Constraining properties of rapidly rotating neutron stars using data from heavy-ion collisions

Plamen G. Krastev, Bao-An Li, and Aaron Worley

Department of Physics, Texas A&M University-Commerce, Commerce, TX 75429, U.S.A.

Plamen_Krastev@tamu-commerce.edu, Bao-An_Li@tamu-commerce.edu,
aworley@leo.tamu-commerce.edu

ABSTRACT

Properties, structure, and thermal evolution of neutron stars are determined by the equation of state of stellar matter. Recent data on isospin-diffusion and isoscaling in heavy-ion collisions at intermediate energies as well as the size of neutron skin in ^{208}Pb have constrained considerably the density dependence of the nuclear symmetry energy and, in turn, the equation of state of neutron-rich nucleonic matter. These constraints could provide useful information about the global properties of rapidly rotating neutron stars. Models of rapidly rotating neutron stars are constructed applying several nucleonic equations of state. Particular emphasis is placed on configurations rotating rigidly at 716 and 1122 Hz. The range of allowed hydrostatic equilibrium solutions is determined and tested for stability. The effect of rotation on the internal composition and thermal properties of neutron stars is also examined. At a given rotational frequency, each equation of state yields a range of possible neutron stars configurations restricted by the Keplerian (mass-shedding) limit, corresponding to the maximal circumferential radius, and the limit due to the onset of instabilities with respect to axial-symmetric perturbations, corresponding to the minimal equatorial radius of a stable neutron star model. We show that the mass of a neutron star rotating uniformly at 1122 Hz is between 1.7 and $2.1M_{\odot}$. Central stellar density and proton fraction decrease with increasing rotational frequency with respect to static models, and depending on the exact stellar mass and angular velocity, can drop below the Direct Urca threshold thus closing the fast cooling channel.

Subject headings: dense matter — equation of state — stars: neutron — stars: rotation

1. Introduction

Neutron stars are one of the most exotic objects in the universe. Matter in their cores is compressed to huge densities ranging from the density of normal nuclear matter, $\rho_0 \approx 0.16 fm^{-3}$, to an order of magnitude higher (Glendenning 2000). The number of baryons forming a neutron star is in the order of $A \approx 10^{57}$. Understanding properties of matter under such extreme conditions of density (and pressure) is still far from complete and represents one of the most important but also challenging problems in modern physics.

Strictly speaking, neutron stars are associated with two classes of astrophysical objects (Weber 1999). Pulsars belong to the first class and are generally accepted to be rotating neutron stars. X-ray sources belong to the second class and some of them are neutron stars on close binary orbit with an ordinary star (e.g., Her X-1 and Vela X-1) (Weber 1999). Because of their strong gravitational binding neutron stars can rotate very fast (Bejger et al. 2007). The first millisecond pulsar PSR1937+214, spinning at $\nu = 641 Hz$ (Backer et al. 1982), was discovered in 1982, and during the next decade or so almost every year a new one was reported. In the recent years the situation changed considerably with the discovery of an anomalously large population of millisecond pulsars in globular clusters (Weber 1999), where the density of stars is roughly 1000 times that in the field of the galaxy and which are therefore very favorable sites for formation of rapidly rotating neutron stars which have been spun up by the means of mass accretion from a binary companion. Presently the number of the observed pulsars is close to 2000, and the detection rate is rather high.

In 2006 Hessels et al. (2006) reported the discovery of a very rapid pulsar J1748-2446ad, rotating at $\nu = 716 Hz$ and thus breaking the previous record (of $641 Hz$). However, even this high rotational frequency is too low to affect the structure of neutron stars with masses above $1M_\odot$ (Bejger et al. 2007). Such pulsars belong to the slow-rotation regime since their frequencies are considerably lower than the Kepler (mass-shedding) frequency ν_k . (The mass-shedding, or Kepler, frequency is the highest possible frequency for a star before it starts to shed mass at the equator.) Neutron stars with masses above $1M_\odot$ enter the rapid-rotation regime if their rotational frequencies are higher than $1000 Hz$ (Bejger et al. 2007). A recent report by Kaaret et al. (2007) suggests that the X-ray transient XTE J1739-285 contains the most rapid pulsar ever detected rotating at $\nu = 1122 Hz$. This discovery has reawakened the interest in building models of rapidly rotating neutron stars (Bejger et al. 2007).

Since neutron stars are objects of extremely condensed matter, the geometry of space-time is considerably altered from that of a flat space. Therefore, the construction of realistic models of neutron stars has to be done in the framework of General Relativity (Weber 1999; Glendenning 2000). Detailed knowledge of the equation of state (EOS) of stellar matter over a very wide range of densities is required for solving the neutron-

star structure equations. At present time the behavior of matter under extreme densities such as those found in the interiors of neutron stars is still highly uncertain and relies upon, often, rather controversial theoretical predictions. Fortunately, heavy-ion reactions provide a unique means to constrain the EOS of dense nuclear matter in terrestrial laboratories (Danielewicz et al. 2002). In particular, one of the main sources of uncertainty in the stellar matter EOS is the density dependence of the nuclear symmetry energy (Lattimer & Prakash 2004; Steiner et al. 2005; Krastev & Sammarruca 2006), $e_{sym}(\rho)$, which is the difference between the energies of pure neutron and symmetric nuclear matter. Due to its importance for the neutron star structure determining the density dependence of the nuclear symmetry energy has been a priority goal for the intermediate energy heavy-ion community. Although extracting the symmetry energy is not an easy task due to the complicated role of the isospin degree of freedom in reaction dynamics, several promising probes of the symmetry energy have been suggested (Li et al. 1997; Li 2000, 2002; Li et al. 1998) (see also (Li & Udo Schroeder 2001; Danielewicz et al. 2002; Baran et al. 2005) for reviews). Some significant progress have been made recently in determining the density dependence of e_{sym} at subsaturation densities using: (1) isospin diffusion (Tsang et al. 2004) and isoscaling (Tsang et al. 2001; Shetty, Yennello & Souliotis 2007) in heavy-ion reactions at intermediate energies (Shi & Danielewicz 2003; Chen et al. 2005; Steiner & Li 2005; Li & Chen 2005), and (2) sizes of neutron skins in heavy nuclei (Steiner et al. 2005; Horowitz & Piekarewicz 2001, 2002; Todd-Rutel & Piekarewicz 2005). At supranormal densities, a number of potential probes of the symmetry energy have been proposed although there is not much data available yet (Chen et al. 2007).

While global properties of spherically symmetric static (non-rotating) neutron stars have been studied extensively (Lattimer & Prakash 2000, 2004; Prakash et al. 2001; Yakovlev & Pethick 2004; Heiselberg & Pandharipande 2000; Heiselberg & Hjorth-Jensen 2000; Steiner et al. 2005; Krastev & Sammarruca 2006), properties of (rapidly) rotating neutron stars have been investigated to lesser extent. Models of (rapidly) rotating neutron stars have been constructed only by several research groups with various degree of approximation (Hartle 1967; Hartle & Thorne 1968; Friedman et al. 1986; Bombaci et al. 2000; Lattimer et al. 1990; Komatsu et al. 1989; Cook et al. 1994; Stergioulas & Friedman 1995, 1998; Bonazzola et al. 1993, 1998; Weber 1999; Ansorg et al. 2002) (see Stergioulas (2003) for a review). In this paper we combine recently obtained data on isospin diffusion, information from flow observables, studies of neutron skin data of ^{208}Pb and other information to constrain global properties of rotating neutron stars. Applying several nucleonic equations of state and the RNS^1 code developed

¹Thanks to Nikolaos Stergioulas the RNS code is available as a public domain program at <http://www.gravity.phys.uwm.edu/rns/>

and made available to the public by Nikolaos Stergioulas (Stergioulas & Friedman 1995), we construct one-parameter 2-D stationary configurations of rapidly rotating neutron stars. The computation solves the hydrostatic and Einstein field equations for mass distributions rotating rigidly under the assumptions of stationary and axial symmetry about the rotational axis, and reflection symmetry about the equatorial plane. This work is organized in the following way: after the introduction in Section 1, we review briefly the structure equations of both static and rotating neutron stars on Section 2. Our numerical results are presented and discussed in Section 3. We conclude with a short summary in Section 4.

2. Equations of neutron star structure

In what follows we present a brief review of structure equations of both static and rotating neutron stars. As already mentioned in the introduction neutron stars are objects of extremely compressed matter and therefore proper understanding of their properties requires application of both General Relativity and the theories of dense matter, which constitute nuclear and particle physics problem. In this respect neutron stars provide a direct link between two of the frontiers of modern physics - General Relativity and strong interactions in dense matter (Weber 1999). The connection between both branches of physics is provided by Einstein’s field equations

$$G^{\mu\nu} = R^{\mu\nu} - \frac{1}{2}g^{\mu\nu}R = 8\pi T^{\mu\nu}(\epsilon, P(\epsilon)), \quad (1)$$

($\mu, \nu = 0, 1, 2, 3$) which couple the Einstein curvature tensor, $G^{\mu\nu}$, to the energy-momentum tensor,

$$T^{\mu\nu} = (\epsilon + P)u^\mu u^\nu + P g^{\mu\nu}, \quad (2)$$

of stellar matter. In the above equations P and ϵ denote pressure and mass energy density, while $R^{\mu\nu}$, $g^{\mu\nu}$, and R denote the Ricci tensor, the metric tensor, and the Ricci scalar curvature respectively (see e.g., Glendenning 2000). In Eq. (2) u^μ is the unit time-like four-velocity satisfying $u^\mu u_\mu = -1$. The tensor $T^{\mu\nu}$ contains the EOS of stellar matter in the form $P(\epsilon)$. In general, Einstein’s field equations and those of the nuclear many-body problem were to be solved simultaneously since the baryons and quarks follow the geodesics of the curved space-time whose geometry, determined by the Einstein’s field equations, is coupled to the total mass energy density of matter (Weber 1999). In the case of neutron stars, as for all astrophysical situations for which the long-range gravitational force can be separated from the short-range strong force, the deviation from flat space-time at the length-scale of the strong interactions ($\sim 1fm$) is practically zero up to the highest densities achieved in the neutron star interiors. (This is not to be confused with the global length-scale of neutron

stars ($\sim 10km$) for which $M/R \sim 0.3$ depending on the star’s mass (in units $c = G = 1$ so that $M_{\odot} \approx 1.475km$.) In other words, gravity curves space-time only on a macroscopic scale but to a very good approximation leaves it flat on a microscopic scale. To achieve an appreciable curvature on a microscopic level at which the strong interactions dominate the particle dynamics mass densities greater than $\sim 10^{40}g\text{ cm}^{-3}$ would be necessary (Weber 1999; Thorne 1966). Under this circumstances the problem of constructing models of neutron stars separates into two distinct tasks. First, the short-range effects of the nuclear forces are described by the principles of many-body nuclear physics in a local inertial frame (co-moving proper reference frame) in which space-time is flat. Second, the coupling between the long-range gravitational force and matter is accounted for by solving the general relativistic equations for the gravitational field described by the curvature of space-time, leading to the global structure of stellar configurations.

2.1. Static stars

In the case of spherically symmetric static (non-rotating) stars the metric has the famous Schwarzschild form:

$$ds^2 = -e^{2\phi(r)} dt^2 + e^{2\Lambda(r)} dr^2 + r^2(d\theta^2 + \sin^2\theta d\phi^2), \quad (3)$$

($c = G = 1$) where the metric functions $\phi(r)$ and $\Lambda(r)$ are given by:

$$e^{2\Lambda(r)} = (1 - \gamma(r))^{-1}, \quad (4)$$

$$e^{2\phi(r)} = e^{-2\Lambda(r)} = (1 - \gamma(r)) \quad r > R_{star}, \quad (5)$$

with

$$\gamma(r) = \begin{cases} \frac{2m(r)}{r} & \text{if } r < R_{star} \\ \frac{2M}{r} & \text{if } r > R_{star} \end{cases} \quad (6)$$

For a static star Einstein’s field equations (Eq. (1)) reduce then to the familiar Tolman-Oppenheimer-Volkoff equation (TOV) (Tolman 1939; Oppenheimer & Volkoff 1939):

$$\frac{dP(r)}{dr} = -\frac{\epsilon(r)m(r)}{r^2} \left[1 + \frac{P(r)}{\epsilon(r)} \right] \left[1 + \frac{4\pi r^3 p(r)}{m(r)} \right] \left[1 - \frac{2m(r)}{r} \right]^{-1} \quad (7)$$

where the gravitational mass within a sphere of radius r is determined by

$$\frac{dm(r)}{dr} = 4\pi\epsilon(r)r^2 dr \quad (8)$$

The metric function $\phi(r)$ is determined through the following differential equation:

$$\frac{d\phi(r)}{dr} = -\frac{1}{\epsilon(r) + P(r)} \frac{dP(r)}{dr}, \quad (9)$$

with the boundary condition at $r = R$

$$\phi(r = R) = \frac{1}{2} \ln \left(1 - \frac{2M}{R} \right) \quad (10)$$

To proceed to the solution of these equations, it is necessary to provide the EOS of stellar matter in the form $P(\epsilon)$. Starting from some central energy density $\epsilon_c = \epsilon(0)$ at the center of the star ($r = 0$), and with the initial condition $m(0) = 0$, the above equations can be integrated outward until the pressure vanishes, signifying that the stellar edge is reached. Some care should be taken at $r = 0$ since, as seen above, the TOV equation is singular there. The point $r = R$ where the pressure vanishes defines the radius of the star and $M = m(R) = 4\pi \int_0^R \epsilon(r') r'^2 dr'$ its gravitational mass.

For a given EOS, there is a unique relationship between the stellar mass and the central density ϵ_c . Thus, for a particular EOS, there is a unique sequence of stars parameterized by the central density (or equivalently the central pressure $P(0)$).

2.2. Rotating stars

Equations of stellar structure of (rapidly) rotating neutron stars are considerably more complex than those of spherically symmetric stars (Weber 1999). These complications arise due to the rotational deformations in rotating stars (i.e., flattening at the poles and bulging at the equator), which lead to a dependence of the star's metric on the polar coordinate θ . In addition, rotation stabilizes the star against gravitational collapse and therefore rotating neutron stars are more massive than static ones. A larger mass, however, causes greater curvature of space-time. This renders the metric functions frequency-dependent. Finally, the general relativistic effect of dragging the local inertial frames implies the occurrence of an additional non-diagonal term, $g^{t\phi}$, in the metric tensor $g^{\mu\nu}$. This term imposes a self-consistency condition on the stellar structure equations, since the degree at which the local inertial frames are dragged along by the star, is determined by the initially unknown stellar properties like mass and rotational frequency (Weber 1999).

Here we outline briefly the equations solved by the *RNS* code. The coordinates of the stationary, axial symmetric space-time used to model a (rapidly) rotating neutron star are

defined through a generalization of Bardeen’s metric (Stergioulas 2003):

$$\begin{aligned}
 ds^2 &= -e^{\gamma+\rho}dt^2 + e^{2\alpha}(dr^2 + r^2d\theta^2) \\
 &+ e^{\gamma-\rho}r^2\sin^2\theta(d\phi - \omega dt^2),
 \end{aligned}
 \tag{11}$$

where the metric potentials γ , ρ , α , and the angular velocity of the stellar fluid relative to the local inertial frame, ω , are functions of the quasi-isotropic radial coordinates, r , and the polar angle θ only. The matter inside a rigidly rotating star is approximated as a perfect fluid (Stergioulas 2003), whose energy momentum tensor is given by Eq. (2). The proper velocity of matter, v , relative to the local Zero Angular Momentum Observer (ZAMO) (Ouyed 2002) is defined as

$$v = r \sin(\theta)(\Omega - \omega)e^{-\rho(r)} \tag{12}$$

with $\Omega = u^3/u^0$ the angular velocity of a fluid element. The four-velocity is given by

$$u^\mu = \frac{e^{-(\gamma+\rho)/2}}{\sqrt{(1-v^2)}}(1, 0, 0, \Omega) \tag{13}$$

In the above equation the function $(\gamma + \rho)/2$ represents the relativistic generalization of the Newtonian gravitational potential, while $\exp[(\gamma + \rho)/2]$ is a time dilation factor between an observer moving with angular velocity ω and one at infinity. Substitution of Eq. (13) into Einstein’s fields equations projected onto the ZAMO reference frame gives three elliptic partial differential equations for the metric potentials γ , ρ , and ω , and two linear ordinary differential equations for the metric potential α . Technically, the elliptic differential equations for the metric functions are converted into integral equations which are then solved iteratively applying Green’s function approach (Komatsu et al. 1989; Stergioulas 2003).

From the relativistic equations of motion, the equations of hydrostatic equilibrium for a barotropic fluid may be obtained as (Stergioulas 2003; Ouyed 2002):

$$h(P) - h_p = \frac{1}{2}[\omega_p + \rho_p - \gamma - \rho - \ln(1 - v^2) + A^2(\omega - \Omega_c)^2], \tag{14}$$

with $h(P)$ the specific enthalpy, P_p the re-scaled pressure, h_p the specific enthalpy at the pole, γ_p and ρ_p the values of the metric potentials at the pole, $\Omega_c = r_e\Omega$, and A a rotational constant (Stergioulas 2003). The subscripts p , e , and c label the corresponding quantities at the pole, equator and center respectively. The *RNS* code solves iteratively the integral equations for ρ , γ and ω , and the ordinary differential equation for the metric function α coupled with Eq. (14) and the equations for hydrostatic equilibrium at the stellar center and equator (given $h(P_c)$ and $h(P_e) = 0$) to obtain ρ , γ , α , ω , the equatorial coordinate radius r_e , angular velocity Ω , energy density ϵ , and pressure P throughout the star.

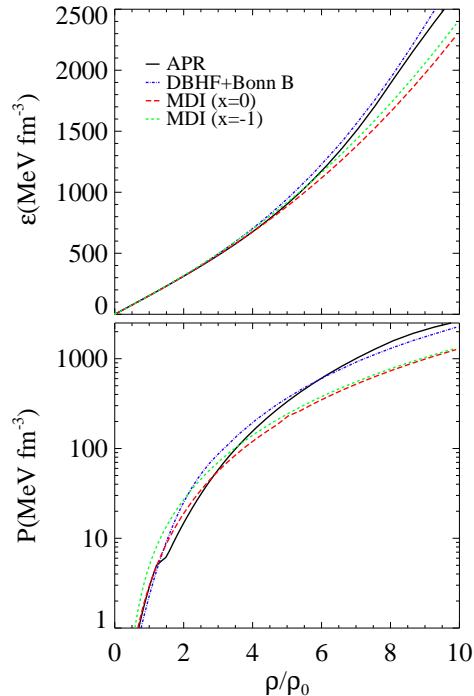


Fig. 1.— (Color online) Equation of state. The upper frame shows the mass energy density as a function of baryon density (in units of ρ_0) and the lower frame shows the total pressure (including the lepton contributions) versus baryon density. (The “dip” exhibited by the density curve of the APR EOS is due to a phase transition from low density phase (LDP) to high density phase (HDP). See (Akmal et al. 1998) for details.)

3. Results and discussion

We compute properties of (rapidly) rotating neutron stars employing several nucleonic EOSs and the *RNS* code. The EOSs applied here are shown in Fig. 1. We pay particular attention to the EOS computed with the MDI interaction (Das et al. 2003) since its symmetry energy is constrained in the sub-saturation density region by the available nuclear laboratory data. The EOS of symmetric nuclear matter for the MDI interaction is constrained up to five times the normal nuclear matter density by the available data on collective flow in relativistic heavy-ion collisions. The parameter x is introduced in the single-particle potential of the MDI EOS to reflect the largely uncertain density dependence of the nuclear symmetry energy $e_{sym}(\rho)$ as predicted by various many-body approaches. Since, as demonstrated by Li & Chen (2005) and Li & Steiner (2006), only equations of state with x between -1 and 0 have symmetry energies consistent with the isospin diffusion data and measurements of the skin thickness of ^{208}Pb , we thus consider only these

two limiting cases as boundaries of the possible rotating neutron star models. Moreover, it is interesting to note that the symmetry energy extracted very recently from the isoscaling analyses of heavy-ion reactions is consistent with the MDI calculation using $x = 0$ (Shetty, Yennello & Souliotis 2007). The MDI EOS has been recently applied to constrain the neutron-star radius (Li & Steiner 2006) with a suggested range compatible with the best estimates from observations. In addition, it has been also used to constrain a possible time variation of the gravitational constant G (Krastev & Li 2007) via the gravitochemical heating formalism developed by Jofre et al. (2006). In Fig. 1 we also show results by Akmal et al. (1998) with the $A18 + \delta v + UIX^*$ interaction (APR) and recent Dirac-Brueckner-Hartree-Fock (DBHF) calculations (Alonso & Sammarruca 2003; Krastev & Sammarruca 2006) with Bonn B One-Boson-Exchange (OBE) potential (DBHF+Bonn B) (Machleidt et al. 1987). Below the baryon density of approximately $0.07 fm^{-3}$ the equations of state shown in Fig. 1 are supplemented by a crustal EOS, which is more suitable for the low density regime. Namely, we apply the EOS by Pethick, Ravenhall & Lorenz (1995) for the inner crust and the one by Haensel & Pichon (1994) for the outer crust. At the highest densities we assume a continuous functional for the EOSs employed in this work. (See (Krastev & Sammarruca 2006) for a detailed description of the extrapolation procedure for the DBHF+Bonn B EOS.) The saturation properties of the nuclear equations of state used in this paper are summarized in Table 1.

Table 1: Saturation properties of the nuclear EOSs (for symmetric nuclear matter) shown in Fig. 1.

EOS	$\rho_0(fm^{-3})$	$E_s(MeV)$	$\kappa(MeV)$	$e_{sym}(\rho_0)(MeV)$	$m^*(\rho_0)/m$
MDI($x=0$)	0.160	-16.08	211.00	31.62	0.67
MDI($x=-1$)	0.160	-16.08	211.00	31.62	0.67
APR	0.160	-16.00	266.00	32.60	0.70
DBHF+Bonn B	0.185	-16.14	259.04	33.71	0.65

The first column identifies the equation of state. The remaining columns exhibit the following quantities at the nuclear saturation density: saturation (baryon) density; energy-per-particle; compression modulus; symmetry energy; nucleon effective mass to *average* nucleon mass ratio (with $m = 938.926 MeV c^{-2}$).

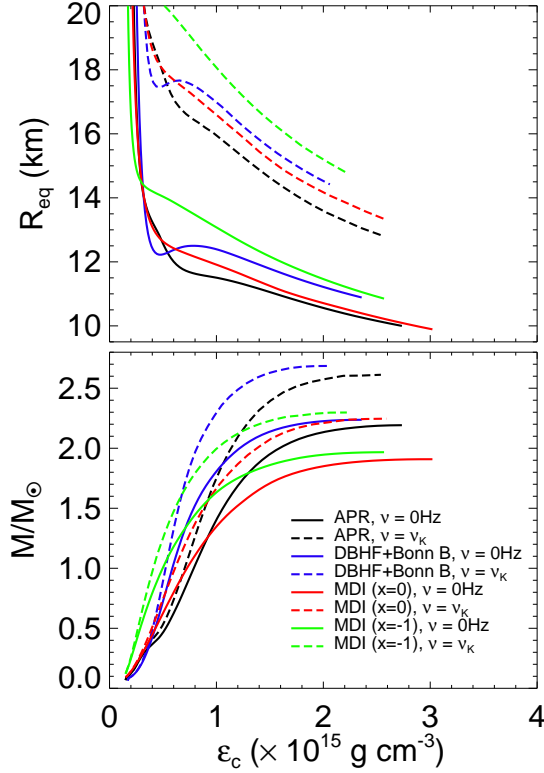


Fig. 2.— (Color online) Neutron star masses and radii. Neutron star equatorial radii (upper panel) and total gravitational mass (lower panel) versus central energy density ϵ_c . Both static (solid lines) and Keplerian (broken lines) models are shown.

3.1. Keplerian (and static) sequences

In what follows we examine the effect of ultra-fast rotation at the Kepler frequency on the neutron star gravitational masses and radii. The equilibrium configurations for both static and (rapidly) rotating neutron stars are parameterized in terms of the central mass energy density, $\epsilon_c = \epsilon(0)$ (or equivalently central pressure, $P_c = P(0)$). This functional dependence is shown in Fig. 2, where we display the stellar *equatorial* radius (upper frame) and total gravitational mass (lower frame) versus central energy density for the EOSs applied in this work. Predictions for both static and maximally rotating models are shown. The main feature of the mass-density plot is that there exists a maximum value of the gravitational mass of a neutron star that a given EOS can support (see e.g., Weber 1999). This holds for both static and (rapidly) rotating stars. The sequences shown in Fig. 2 terminate at the “maximum mass” point. Comparing the results for static and rotating stars, it is seen clearly that the rapid rotation increases noticeably the mass that can be supported against

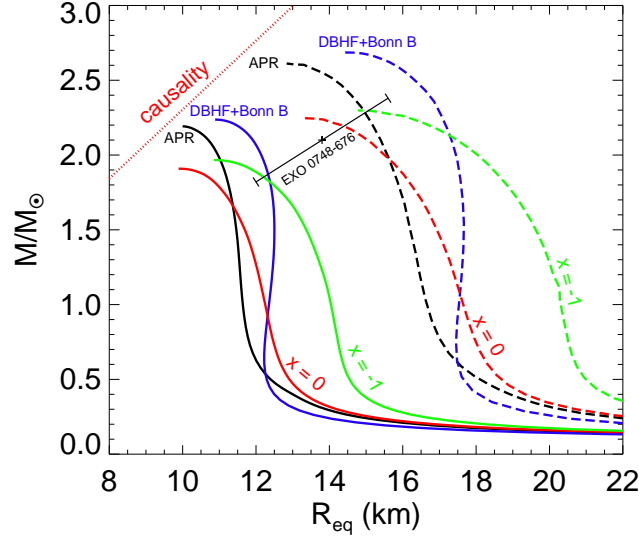


Fig. 3.— (Color online) Mass-radius relation. Both static (solid lines) and Keplerian (broken lines) sequences are shown. The $1 - \sigma$ error bar corresponds to the measurement of the mass and radius of EXO 0748-676 (Ozel 2006).

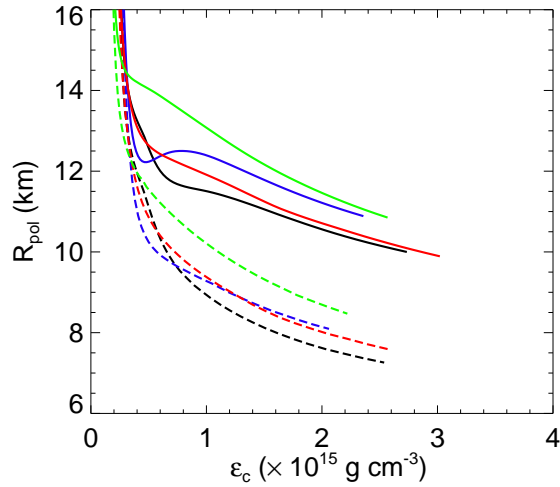


Fig. 4.— (Color online) Neutron-star polar radius versus central energy density. Both static (solid lines) and Keplerian (broken lines) sequences are shown. The labeling of the curves is the same as in Fig. 2.

collapse while lowering the central density of the maximum-mass configuration. This is what one should expect, since, as already mentioned, rotation stabilizes the star against the gravitational pull providing an extra (centrifugal) repulsion. The rotational effect on the mass-radius relation is illustrated in Fig. 3 where the gravitational mass is given as a function

of the circumferential radius. For rapid rotation at the Kepler frequency, a mass increase up to $\sim 17\%$ (Table 3) is obtained, depending on the EOS. The equatorial radius increases by several kilometers, while the polar radius decreases by several kilometers (see Fig. 4) leading to an overall oblate shape of the rotating star. Table 2 summarizes the properties (masses, radii and central energy densities) of the maximum-mass nonrotating neutron star configurations. Our studies on the effect of rapid rotation on the upper mass limits for the four EOSs considered in the present paper are presented in Table 3. In each case the upper mass limit is attained for a model at the mass-shedding limit where $\nu = \nu_k$, with central density $\sim 15\%$ below that of the static model with the largest mass. These findings are consistent with those by Friedman et al. (1984) and Stergioulas & Friedman (1995). Table 3 also provides an estimate of the upper limiting rotation rate of a neutron star. In general, softer EOSs permit larger rotational frequencies since the resulting stellar models are more centrally condensed (see e.g., Friedman et al. 1984). In the last column of Table 3 we show the Kepler frequencies computed via the empirical relation

$$\frac{\Omega_k}{10^4 s^{-1}} = 0.72 \left(\frac{M_s}{M_\odot} \right)^{1/2} \left(\frac{R_s}{10 km} \right)^{-3/2} \quad (15)$$

proposed by Friedman et al. (1989). The uncertainty of Eq. (15) is $\sim 10\%$ (see Haensel & Zdunik (1989) for an improved version of the empirical formula). At the time of constructing the above relation Friedman et al. (1989) did not consider a then unknown class of minimum period EOSs (Stergioulas 1996) which explains why the numbers in the last column of Table 3 exhibit larger deviation from the exact numerical solutions (in column five). This is particularly pronounced for the APR EOS for which the approximated Kepler frequency deviates $\sim 14\%$ from the exact solution. (Note that the APR EOS has the lowest period among the EOSs considered here.)

Fig. 5 displays the neutron star gravitational mass as a function of the Kepler frequency,

Table 2: Maximum-mass static (nonrotating) models.

EOS	$M_{max}(M_\odot)$	$R(km)$	$\epsilon_c(\times 10^{15} g cm^{-3})$
MDI(x=0)	1.91	9.89	3.02
APR	2.19	9.98	2.73
MDI(x=-1)	1.97	10.85	2.57
DBHF+Bonn B	2.24	10.88	2.36

The first column identifies the equation of state. The remaining columns exhibit the following quantities for the static models with maximum gravitational mass: gravitational mass; radius; central mass energy density.

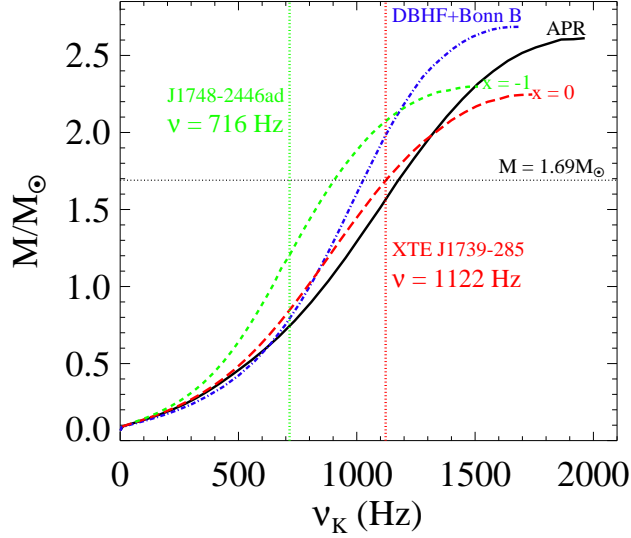


Fig. 5.— (Color online) Mass versus Keplerian (mass-shedding) frequency ν_k .

ν_k . The vertical dotted lines denote the frequencies of the fastest neutron stars - XTE J1739-285 (Kaaret et al. 2007) (red) and J1748-2446ad (Hessels et al. 2006) (green). From this figure one can conclude that only neutron stars with masses above approximately $1.7M_\odot$ can rotate at $\nu = 1122Hz$ (and/or faster). We discuss this further in the next subsection (3.2).

Table 3: Maximum-mass rapidly rotating models at the Kepler frequency $\nu = \nu_k$.

EOS	$M_{max}(M_\odot)$	Increase (%)	$\epsilon_c(\times 10^{15}g\text{ cm}^{-3})$	$\nu_k(Hz)$	$\nu_k^{FIP}(Hz)$
MDI(x=0)	2.25	15	2.59	1742	1610
APR	2.61	17	2.53	1963	1699
MDI(x=-1)	2.30	14	2.21	1512	1423
DBHF+Bonn B	2.69	17	2.06	1685	1510

The first column identifies the equation of state. The remaining columns exhibit the following quantities for the maximally rotating models with maximum gravitational mass: gravitational mass; its percentage increase over the maximum gravitational mass of static models; central mass energy density; maximum rotational frequency; Kepler frequency as computed via the empirical relation by.

3.2. Rotation at 716 and 1122 Hz

In this subsection we study neutron stars rotating at 716 (Hessels et al. 2006) and 1122 Hz (Kaaret et al. 2007) which are the rotational frequencies of the fastest pulsars as of today. Stability with respect to the mass-shedding from equator implies that at a given gravitational mass the equatorial radius R_{eq} should be smaller than R_{eq}^{max} corresponding to the Keplerian limit (Bejger et al. 2007). The value of R_{eq}^{max} results from the condition that the frequency of a test particle at circular equatorial orbit of radius R_{eq}^{max} just above the equator of the actual rotating star is equal to the rotational frequency of the star. As reported by (Bejger et al. 2007) the relation between M and R_{eq} at the “mass-shedding point” is very well approximated by the expression for the orbital frequency for a test particle orbiting at $r = R_{eq}$ in the Schwarzschild space-time created by a spherical mass. The formula satisfying $\nu_{orb}^{Schw.} = \nu$, represented by the dotted line in Figs. 6 and 7, is given by

$$\frac{1}{2\pi} \left(\frac{GM}{R_{eq}^3} \right) = \nu, \quad (16)$$

where $\nu = 716Hz$ in Fig. 6 and $\nu = 1122Hz$ in Fig. 7 respectively. This formula for the Schwarzschild metric coincides with the one obtained in Newtonian gravity for a point mass M (Bejger et al. 2007). Eq. (16) implies

$$R_{max} = \chi \left(\frac{M}{1.4M_{\odot}} \right)^{1/3} km, \quad (17)$$

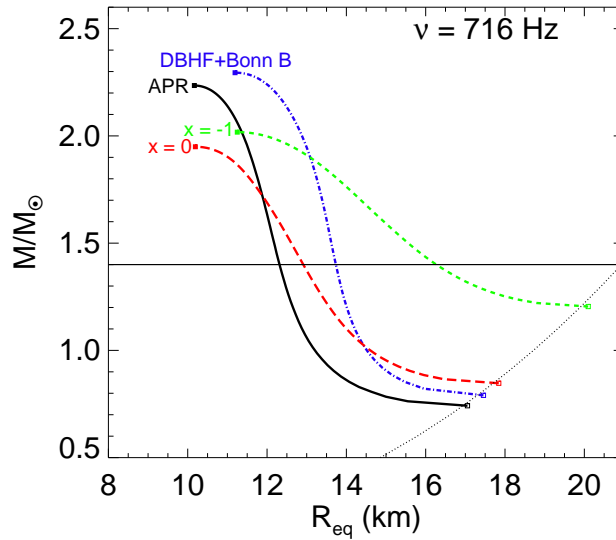


Fig. 6.— (Color online) Gravitational mass versus circumferential radius for neutron stars rotating at $\nu = 716Hz$. See text for details.

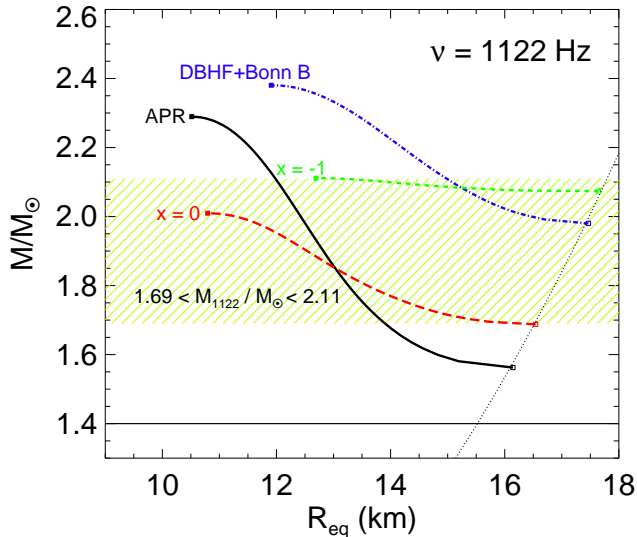


Fig. 7.— (Color online) Gravitational mass versus circumferential radius for neutron stars rotating at $\nu = 1122Hz$.

with $\chi = 20.94$ for rotational frequency $\nu = 716Hz$ (Fig. 6) and $\chi = 15.52$ for $\nu = 1122Hz$ (Fig. 7).

In Figs. 6 and 7 we observe that the range of the allowed masses supported by a given EOS for rapidly rotating neutron stars becomes narrower than the one of static configurations. This effect becomes stronger with increasing frequency and depends upon the EOS. For instance, for models rotating at $1122Hz$ (Fig. 7) for the $x=-1$ EOS the allowed mass range is $\sim 0.1M_{\odot}$. Since predictions from the $x=0$ and $x=-1$ EOSs represents the limits of the neutron star models consistent with the nuclear data from terrestrial laboratories, we conclude that the mass of the neutron star in XTE J1739-285 is between 1.7 and $2.1M_{\odot}$.

3.3. Rotation and proton fraction

Finally, we study the effect of (fast) rotation on the proton fraction in the star core. In Fig. 8 we show the central baryon density (upper frame) and central proton fraction (lower frame) as a function of the rotational frequency for fixed-mass models. Predictions from both $x = 0$ and $x = -1$ EOSs are shown. We observe that central density decreases with increasing frequency. This reduction is more pronounced in heavier neutron stars. Most importantly, we also observe decrease in the proton fraction Y_p^c in the star’s core. We recall that large proton fraction (above ~ 0.14 for $npe\mu$ -stars) leads to fast cooling of neutron stars through direct Urca reactions. Our results demonstrate that depending on the stellar

mass and rotational frequency, the central proton fraction could, in principle, drop below the threshold for the direct *nucleonic* Urca channel and thus making the fast cooling in rotating neutron stars impossible. The masses of the models shown in Fig. 8 are chosen so that the proton fraction in stellar core is just above the direct Urca limit for the *static* configurations, see Fig. 9 upper and lower frames. The stellar sequences in Fig. 8 are terminated at the Kepler (mass-shedding) frequency. In both cases the central proton fraction drops below the direct Urca limit at frequencies lower than that of PSR J1748-244ad (Hessels et al. 2006). This implies that the fast cooling can be effectively blocked in millisecond pulsars depending on the exact mass and spin rate. It might also explain why heavy neutron stars (could) exhibit slow instead of fast cooling. For instance, with the $x = 0$ EOS (with softer symmetry energy) for a neutron star of mass approximately $1.9M_{\odot}$, the Direct Urca channel closes at $\nu \approx 470Hz$. On the other hand, with the $x=-1$ EOS (with stiffer symmetry energy) the direct Urca channel can close only for low mass neutron stars, in fact only for masses well below the canonical mass of $1.4M_{\odot}$. This is due to the much stiffer symmetry energy (see Fig. 9 middle frame) because of which the direct Urca threshold (Fig. 9 lower frame) is reached at much lower densities and stellar masses (Fig. 9 upper frame).

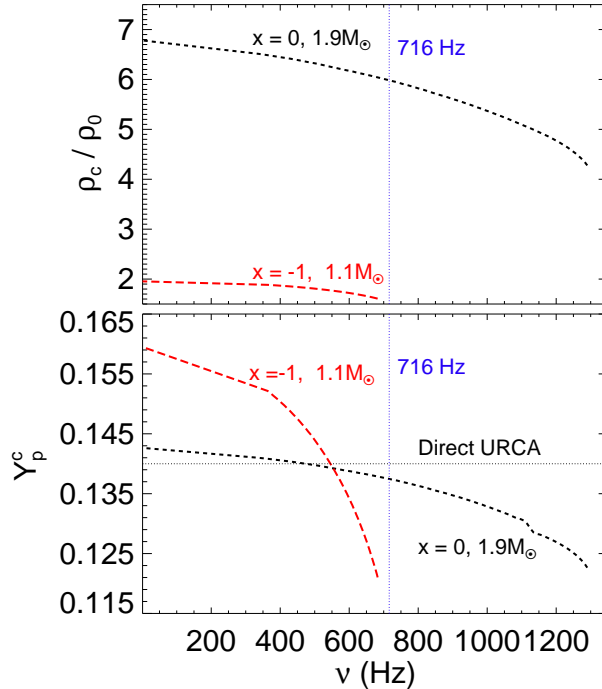


Fig. 8.— (Color online) Density (upper panel) and proton fraction (lower panel) versus rotational frequency for fixed neutron star mass.

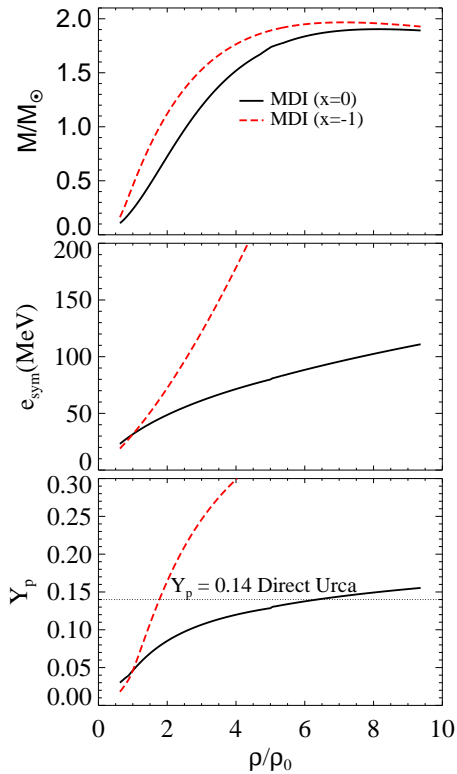


Fig. 9.— (Color online) Neutron star mass (upper panel), nuclear symmetry energy (middle panel) and proton fraction (lower panel) versus baryon density. Predictions from the MDI ($x=-1,0$) are shown.

Before closing the discussion in this section a few comments are in order. In the present study we do not consider "exotic" states of matter in neutron stars. On the other hand, due to the rapid rise of the baryon chemical potentials several other species of particles, such as strange hyperons Λ^0 and Σ^- , are expected to appear once their mass thresholds are reached (Baldo et al. 2000). The appearance of hyperonic degrees of freedom lowers the energy-per-particle in the stellar medium and causes more centrally condensed configurations with lower masses and radii. Additionally, hyperons help the condition for *nucleonic* direct Urca process to be satisfied at lower densities due to the increased proton fraction (Prakash et al. 1992), and depending on their exact concentrations could potentially contribute to the fast cooling of the star through *hyperonic* direct Urca processes (Page et al. 2006). These considerations would alter the balance between the curves in Fig. 9 and ultimately the results displaced in Fig. 8 in favor of the direct Urca process, i.e. smaller masses and higher frequencies would be necessary to close the fast cooling channel. This is due to the fact that the overall impact of (rapid) rotation on the neutron star structure is smaller

for more centrally condensed models resulting from “softer” EOSs (Friedman et al. 1984). Therefore, for such models there is smaller deviation from properties and structure of static configurations. In addition, at even higher densities matter is expected to undergo a transition to quark-gluon plasma (Weber 1999; Baldo et al. 2000), which favors a fast cooling through enhanced nucleonic direct Urca and quark direct Urca processes (see e.g., Page et al. 2006).

4. Summary

We have studied properties of (rapidly) rotating neutron stars employing four nucleonic EOSs. Rapid rotation affects the neutron star structure significantly. It increases the maximum possible mass up to $\sim 17\%$ and increases/decreases the equatorial/polar radius by several kilometers. Our findings, through the application of EOSs with constrained symmetry energy by recent nuclear terrestrial laboratory data, allowed us to constrain the mass of the neutron star in XTE J1739-285 to be between 1.7 and $2.1M_{\odot}$.

Additionally, rotation reduces central density and proton fraction in the neutron star core, and depending on the exact stellar mass and rotational frequency could effectively close the fast cooling channel in millisecond pulsars. This circumstance may have important consequences for both the interpretation of cooling data and the thermal evolution modeling.

Acknowledgements

We would like to thank Nikolaos Stergioulas for making the RNS code available. We also thank Wei-Zhou Jiang for helpful discussions. This work was supported by the National Science Foundation under Grant No. PHY0652548 and the Research Corporation under Award No. 7123.

REFERENCES

- Akmal, A., Pandharipande, V. R., & Ravenhall, D. G. 1998, *Phys. Rev.*, C58, 1804
- Alonso, D. & Sammarruca, F. 2003, *Phys. Rev.*, C67, 054301
- Ansorg, M., Kleinwächter, A., & Meinel, R. 2002, *A&A*, 381, L49
- Backer, D. C., Kulkarni, S. R., Heiles, C., et al. 1982, *Nature*, 300, 615

- Baldo, M., Burgio, G. F., & Schulze, H.-J. 2000, *Phys. Rev. C*, 61, 055801
- Baran, V., Colonna, M., Greco, V., & Di Toro, M. 2005, *Phys. Rept.*, 410, 335
- Bejger, M., Haensel, P., & Zdunik, J. L. 2007, *A&A*, 464, L49
- Bombaci, I., Thampan, A. V., & Datta, B. 2000, *Astrophys. J.*, 541, L71
- Bonazzola, S., Gourgoulhon, E., & Marck, J.-A. 1998, *Phys. Rev. D*, 58, 104020
- Bonazzola, S., Gourgoulhon, E., Salgado, M., & Marck, J. A. 1993, *A&A*, 278, 421
- Chen, L. W., Ko, C. M., & Li, B.-A. 2005, *Phys. Rev. Lett.*, 94, 032701
- Chen, L. W., Ko, C. M., Li, B. A., Yong, G. C., 2007, *Frontiers of Physics in China* 2, 327.
- Cook, G. B., Shapiro, S. L., & Teukolsky, S. A. 1994, *ApJ*, 424, 823
- Danielewicz, P., Lacey, R., & Lynch, W. G. 2002, *Science*, 298, 1592
- Das, C. B., Gupta, S. D., Gale, C., & Li, B.-A. 2003, *Phys. Rev.*, C67, 034611
- Friedman, J. L., Parker, L., & Ipser, J. R. 1984, *Nature*, 312, 255
- Friedman, J. L., Parker, L., & Ipser, J. R. 1986, *Astrophys. J.*, 304, 115
- Friedman, J. L., Ipser, J. R., & Parker, L. 1989, *Phys. Rev. Lett.*, 62, 3015
- Glendenning, N. K. 2000, *Compact Stars, Nuclear Physics, Particle Physics, and General Relativity* (New York: Springer-Verlag)
- Haensel, P. & Zdunik, J. L. 1989, *Nature*, 340, 617
- Haensel, P. & Pichon, B. 1994, *Astron. Astrophys.*, 283, 313
- Hartle, J. B. 1967, *Astrophys. J.*, 150, 1005
- Hartle, J. B. & Thorne, K. S. 1968, *Astrophys. J.*, 153, 807
- Heiselberg, H. & Hjorth-Jensen, M. 2000, *Phys. Rept.*, 328, 237
- Heiselberg, H. & Pandharipande, V. 2000, *Ann. Rev. Nucl. Part. Sci.*, 50, 481
- Hessels, J. W. T., Ransom, S. M., Stairs, I. H., et al. 2006, *Science*, 311, 1901
- Horowitz, C. J. & Piekarewicz, J. 2001, *Phys. Rev. Lett.*, 86, 5647

- Horowitz, C. J. & Piekarewicz, J. 2002, *Phys. Rev.*, C66, 055803
- Jofre, P., Reisenegger, A., & Fernandez, R. 2006, *Phys. Rev. Lett.*, 97, 131102
- Kaaret, P., Prieskorn, J., in't Zand, J. J. M., et al. 2007, *Astrophys. J.*, 657, L97
- Komatsu, H., Eriguchi, Y., & Hachisu, I. 1989, *MNRAS*, 237, 355
- Krastev, P. G. & Li, B.-A. 2007, *Phys. Rev.* C76, 055804
- Krastev, P. G. & Sammarruca, F. 2006, *Phys. Rev.*, C74, 025808
- Lattimer, J. M. & Prakash, M. 2000, *Phys. Rept.*, 333, 121
- Lattimer, J. M. & Prakash, M. 2004, *Science*, 304, 536
- Lattimer, J. M., Prakash, M., Masak, D., & Yahil, A. 1990, *ApJ*, 355, 241
- Li, B.-A. 2000, *Phys. Rev. Lett.*, 85, 4221
- Li, B.-A. 2002, *Phys. Rev. Lett.*, 88, 192701
- Li, B.-A. & Chen, L.-W. 2005, *Phys. Rev.*, C72, 064611
- Li, B.-A., Ko, C. M., & Bauer, W. 1998, *Int. J. Mod. Phys.*, E7, 147
- Li, B.-A., Ko, C. M., & Ren, Z.-Z. 1997, *Phys. Rev. Lett.*, 78, 1644
- Li, B.-A. & Steiner, A. W. 2006, *Phys. Lett.*, B642, 436
- Li, B. A. & Udo Schroeder, W. 2001, *Isospin Physics in Heavy-Ion Collisions at Intermediate Energies* (New York: Nova Science)
- Machleidt, R., Holinde, K., & Elster, C. 1987, *Phys. Rept.*, 149, 1
- Oppenheimer, J. R. & Volkoff, G. M. 1939, *Phys. Rev.*, 55, 374
- Ouyed, R. 2002, *A&A*, 382, 939
- Ozel, F. 2006, *Nature*, 441, 1115
- Page, D., Geppert, U., & Weber, F. 2006, *Nucl. Phys.*, A777, 497
- Pethick, C. J., Ravenhall, D. G., & Lorenz, C. P. 1995, *Nucl. Phys.*, A584, 675
- Prakash, M., Lattimer, J. M., Sawyer, R. F., & Volkas, R. R. 2001, *Ann. Rev. Nucl. Part. Sci.*, 51, 295

- Prakash, M., Prakash, M., Lattimer, J. M., & Pethick, C. J. 1992, ApJ, 390, L77
- Shetty, D., Yennello, S.J. and Souliotis, G.A., 2007, Phys. Rev. C75, 034602.
- Shi, L. & Danielewicz, P. 2003, Phys. Rev., C68, 064604
- Steiner, A. W. & Li, B.-A. 2005, Phys. Rev., C72, 041601
- Steiner, A. W., Prakash, M., Lattimer, J. M., & Ellis, P. J. 2005, Phys. Rept., 411, 325
- Stergioulas, N. 1996, Doctoral Dissertation, The University of Wisconsin-Milwaukee
- Stergioulas, N. 2003, Living Rev. Rel., 6, 3
- Stergioulas, N. & Friedman, J. L. 1995, Astrophys. J., 444, 306
- Stergioulas, N. & Friedman, J. L. 1998, Astrophys. J., 492, 301
- Thorne, K. S. 1966, in: *Proc. Int. School of Phys. "Enrico Fermi"*, Course 35, High Energy Astrophysics, ed. by L. Gratton (New York: Academic Press)
- Todd-Rutel, B. G. & Piekarewicz, J. 2005, Phys. Rev. Lett., 95, 122501
- Tolman, R. C. 1939, Phys. Rev., 55, 364
- Tsang, M.B. et al., 2001, Phys. Rev. Lett. 86, 5023.
- Tsang, M.B. et al., 2004, Phys. Rev. Lett. 92, 062701.
- Weber, F. 1999, Pulsars as Astrophysical Laboratories for Nuclear and Particle Physics (Bristol, Great Britan: IOP Publishing)
- Yakovlev, D. G. & Pethick, C. J. 2004, Ann. Rev. Astron. Astrophys., 42, 169